ASTROCYTE REACTIVITY CHARACTERIZED WITH MONOCLONAL

ANTIBODY J1-31: AN EVALUATION OF cAMP EFFECTORS

THESIS

Presented to the Graduate Council of
Texas State University – San Marcos
in Partial Fulfillment
of the Requirements

for the Degree

Master of SCIENCE

by

Sarah J. Kane, B.S

San Marcos, Texas
August 2012

ASTROCYTE REACTIVITY CHARACTERIZED WITH MONOCLONAL

ANTIBODY J1-31: AN EVALUATION OF cAMP EFFECTORS

Committee Members Approved:

_____

Joseph R. Koke, Chair

_____

Dana M. García

_____

Shannon E. Weigum

Approved:

_____

J. Michael Willoughby
Dean of the Graduate College

FAIR USE AND AUTHOR'S PERMISSION STATEMENT

Fair Use

Duplication Permission

ACKNOWLEDGEMENTS

TABLE OF CONTENTS

Page

CHAPTER

LIST OF TABLES

LIST OF FIGURES

ABSTRACT

ASTROCYTE REACTIVITY CHARACTERIZED WITH MONOCLONAL

ANTIBODY J1-31: AN EVALUATION OF cAMP EFFECTORS

by

Sarah Jo Kane, B.S.

Texas State University-San Marcos

August 2012

SUPERVISING PROFESSOR: JOSEPH R. KOKE

Apart from the embryonic stage, regeneration of the central nervous system (CNS) following injury in higher vertebrates is limited if not precluded entirely. This inability of neurons in the CNS to regenerate is at least partially attributed to the transition of astrocytes, a supportive cell type in the CNS, to a reactive state in response to injury, which may lead to the formation of a glial scar. The most well characterized indicator of reactive astrocytes is increased labeling of glial fibrillary acidic protein (GFAP), a structural component of the astrocytic cytoskeleton (Faulkner et al. 2004, Geisert et al. 1990, Hausmann et al. 2000, Tetzlaff 1988, among others). Interestingly, when GFAP and another cytoskeletal protein,

vimentin, were knocked out in a mouse model, regenerative capabilities were evident after spinal cord injury (Menet et al. 2003). This study has given researchers the notion that cytoskeletal elements may be one of the components responsible for the lack of regeneration in mammals after CNS insults.

Astrocytes have a broad range of functions in the CNS, although the role of reactive astrocytes, whether positive or negative with respect to neuronal growth/regrowth, has been debated among researchers for years. Selectively abolishing proliferative reactive astrocytes altogether has a negative effect (Myer et al. 2006, Sofroniew et al. 2005), with degeneration seen far past the injury site. Reactive astrocytes normally demarcate the injury site, ensuring degeneration only occurs within the restricted area. However, highly reactive astrocytes begin forming a glial scar, which presents a fibrous network impeding axonal regeneration, remyelination, or both, following insults to the CNS.

The dual role, both friend and foe, of these reactive cells piques an interest not in determining how to rid systems of reactive astrocytes entirely, but rather in targeting molecules and proteins involved in the scar-producing aspect of reactivity without inhibiting the positive role that reactive astrocytes may play. Cyclic adenosine monophosphate (cAMP) is a secondary messenger that has been shown to increase GFAP expression and stellated morphology in several studies of astrocytes (Fedoroff et al. 1984, Lee et al. 1997). In order to determine the downstream effector(s) of cAMP involved in the transition to reactivity, specific activators and/or inhibitors of downstream pathways were utilized in this study. The marker of reactivity was increased immunolabeling of monoclonal antibody J1-31 (mAb J1-31), an antibody raised against multiple sclerotic plaques, which recognizes

cytoskeletal elements that are upregulated in reactive astrocytes (Malhotra et al. 1989, Malhotra et al. 1993, Predy et al. 1988).

Treatments activating the guanine nucleotide exchange factor (GEF) directly activated by cAMP, and not the protein kinase A pathway, revealed phenotypes and immunolabeling patterns of mAb J1-31 characteristic of reactive astrocytes. The GEF activated by cAMP is named Exchange protein activated by cAMP (Epac). Additionally, we observed partial, but not complete, colocalization of the J1-31 antigen and GFAP. We thus conclude that labeling of the J1-31 antigen increases in response to the cAMP dependent GEF stimulation, and that the J1-31 antigen is most likely a variant of GFAP as well as other cytoskeletal components.

CHAPTER I

INTRODUCTION

Glial cells were named due to their supportive function, a Greek term which translates to "glue." Glial cells in the central nervous system (CNS) include astrocytes, microglia, and oligodendrocytes. Astrocytes outnumber neurons 5:1 (Sofroniew and Vinters 2010), and are therefore one of the main cell types in the CNS. They play diverse roles, including participation in the formation the blood brain barrier, maintaining ionic balances, aiding in synaptic transmission, initiating immune reaction cascades due to expression of major histocompatibility complexes, and homing into an injury site to repair damage, to name a few (Daginakatte et al. 2007).

The blood brain barrier (BBB) is the collection of a basal membrane, astrocytic end feet, and endothelial cells connected via tight junctions, all of which collectively surround the lumen of blood capillaries and prevent passive diffusion of particles from the blood into the interstitial spaces of the brain. Astrocytes have been reported to be involved in the formation of these endothelial tight junctions, where they were seen to induce non-nervous system endothelial cells to exhibit blood brain barrier properties *in vitro* (Janzer and Raff 1987). These tight junctions are required to separate the CNS from potentially harmful substances in circulating blood. Without the integrity of the BBB, the CNS, a normally sterile environment, becomes susceptible to invading pathogens and toxic molecules.

1

Communication in the brain has been traditionally thought to rely exclusively on neurons. However, astrocytes have been shown to play a major role in ensuring neurons communicate properly. They regulate neuronal function, promote synchronous action of neurons, and ensure proper synaptic transmission (Haydon and Carmignoto 2006). Although astrocytes do not communicate via action potentials like neurons, they do have receptors for a wide range of neurotransmitters and communicate with other cell types, such as meningeal cells, via calcium waves (Grafstein et al. 2000).

When astrocytes respond to damage in the CNS, they undergo a phenotypic and/or mitotic transition coined reactivity. Reactive astrocytes are characterized as being hypertrophic or hyperplasic, in which they undergo cytoskeletal rearrangements and may begin dividing (Silver and Miller 2004). Hypertrophy is defined as cell enlargement and is associated with a drastic increase in intermediate filament production as well as extension of cytoplasmic processes, while hyperplasia is defined as increased proliferation. Both the hypertrophic and hyperplasic responses have been described as mainly restricted to the primary insult site (Ridet et al. 1997, Sofroniew 2005), where the astrocytes nearest the insult site reveal the highest degree of reactivity, and the magnitude of insult determines the magnitude of the reactive response. The most well known indicator of reactive astrocytes is the upregulation of GFAP (Faulkner et al. 2004, Geisert et al. 1990, Hausmann et al. 2000, Tetzlaff 1988, among others), a type III intermediate filament. The roles of reactive astrocytes with respect to axonal regeneration after injury, whether positive or negative, have been debated for years (Buffo et al. 2010).

When an insult to the CNS is of high enough severity, the formation of a glial scar can occur. A glial scar is a complex mixture of reactive astrocytes, other glial cells such as

microglia and oligodendrocyte precursor cells, meningeal cells, as well as extracellular matrix components (Yiu and He 2006). Although the glial scar acts as a blockage to prevent the injury site from further damage from inflammatory white blood cells (Sofroniew 2005), this three-dimensional, fibrous network acts as a physical barrier to regenerating axons. Reactive astrocytes are considered the main component of the glial scar, and are responsible for secreting laminin, fibronectin, and chondroitin sulphate proteoglycans, among other extracellular matrix molecules (Yiu and He 2006). A review by Sofronview and Vinters in 2010 discusses the degrees of the astroglial reactive response, stating that highly reactive astrocytes intertwine processes with multiple reactive astrocytes, a necessary process for the formation of the glial scar. The review also discusses a lesser degree of reactivity that does not result in the formation of the glial scar, where the astrocytes undergo the phenotypic response, yet do not begin overlapping with one another and therefore do not form a scar. The degree of this reactive response is dependent on the magnitude of insult, as well as the response from other cell types.

There are several factors known to be involved in the formation of the glial scar. A review by Silver and Miller in 2004 discusses the role of transforming growth factor β (TGFβ), interleukin-1 (IL-1), interferon-γ (IFNγ), and fibroblast growth factor 2 (FGF2) with respect to the production of the glial scar. TGFβ has been shown to increase production of the extracellular proteoglycans produced by astrocytes. The inflammatory response of reactive astrocytes is mediated through IL-1, IFNγ, and FGF2. When neonatal rat astrocytes were exposed to IL-1, reactivity was observed through increased immunodetection of GFAP (Giulian and Lachman 1985). Although all of these factors are important candidates for understanding how the glial scar is produced, as well as potential

therapeutic targets to aid in regeneration past the glial scar, other signals cueing the morphological changes leading to the astroglial reactive response should be further explored.

In 2005, Sofroniew conducted a critical study for understanding the effects of eliminating reactive astrocytes altogether and also very eloquently discussed the paradoxical nature of reactive astrocytes. A GFAP-TK transgenic mouse line halts DNA synthesis in dividing reactive astrocytes, thereby killing them. These transgenic mice have a viral kinase sequence under the GFAP promoter, the expression of which does not affect normally growing astrocytes. However, when an insult was introduced to the CNS, coupled with delivery of an antiviral agent, the kinase phosphorylates the antiviral agent, which stops DNA synthesis, thereby killing the proliferative astrocytes. This model provided a way to observe the effects of abolishing dividing, reactive astrocytes. After a hippocampal stab wound to a GFAP-TK transgenic mouse, in which reactive dividing astrocytes were ablated, the neighboring, uninjured tissue was also exposed to the inflammatory response, and cellular degeneration far past the injury site was observed, which Sofroniew attributed to glutamate-mediated excitotoxicity. With the presence of reactive astrocytes, the damage site would normally have been separated from uninjured tissue, thereby restricting the inflammatory response to the damaged area. Furthermore, after spinal cord injury, a glial scar was not apparent in the GFAP-TK transgenic line; therefore, the injury site was exposed to pro-inflammatory and secondary degenerative mechanisms, which also resulted in larger amount of degeneration beyond the injury site. Likewise, in a different study, the same transgenic line was injured with a moderate controlled cortical injury, after which the loss of reactive astrocytes revealed increased axonal degeneration and a higher degree of pro-inflammatory cells present at the injury site (Myer et al. 2006). These studies illustrate the

concept that reactive astrocytes can indeed play a positive, protective role following injury to the CNS.

Considering reactive astrocytes do indeed have positive roles following injury to the CNS, targeting specific genes (instead of killing the cells altogether) is of interest. Several studies indicate disrupting the expression of certain cytoskeletal components aids axonal regeneration after injury. For example, when GFAP and vimentin were selectively knocked out in a mouse model, functional recovery was seen after a hemisection of the spinal cord and brain injury (Menet et al. 2003, Pekny et al. 1999). Perhaps without GFAP and vimentin, the glial scar was absent, yet the positive, protective aspects of the astrocytes were still evident.

To ascertain ways to promote such regeneration without generating transgenic organisms, an interest should be taken in molecules known to increase GFAP production in reactive astrocytes. Cyclic adenosine monophosphate (cAMP) is one of these molecules. A 24-hour treatment of cAMP or forskolin caused a significant increase of GFAP mRNA levels and caused astrocytes to become process-bearing (Lee et al. 1997), both of which are indicators of reactivity. Forskolin activates adenylyl cyclase, which converts adenosine tri-phosphate (ATP) to cAMP, thus increasing intracellular levels of cAMP. Likewise, treating primary astrocyte cultures with dibutyryl cAMP (dbcAMP), a membrane permeant analog of cAMP, caused increased immunodetection of GFAP through immunocytochemistry analysis and significantly more GFAP mRNA levels were detected through real-time reverse transcripton-PCR than untreated astrocytes (Daginakatte et al. 2007). Furthermore, other indicators of astrocyte reactivity, such as increased expression of ATF-3 and bystin, are regulated by cAMP (Fang et al. 2008, Neve et al. 2011, Saul et al. 2010).

Cyclic AMP is involved in a wide array of signaling pathways, although in animals only three known downstream targets of cAMP are known: protein kinase A (PKA), exchange protein activated by cAMP (Epac), and cAMP-gated ion channels. Once activated by cAMP, PKA dissociates into four subunits, two of which are catalytically active. The active subunits of PKA phosphorylate proteins, and one of the best characterized downstream target of PKA is a transcription factor, CREB. When activated by cAMP, Epac helps the small GTPases Rap1 and Rap2 exchange guanine diphosphate (GDP) for guanine triphosphate (GTP). When GTP is bound, Rap1 has been shown to aid in the formation of cell junctions. A more detailed description of the roles of Rap1 is given in chapter IV. Cyclic AMP-gated ion channels are triggered to open when cAMP binds to the channel intracellularly.

Although the reactive response induced by cAMP in astrocytes has been reported in numerous publications (see for example Daginakatte et al. 2007, Tokita et al. 2001, Takanaga et al. 2004), the role of cAMP in axonal regrowth after injury has been a contradictorily reported among researchers for years. Cai et al. 2001 discuss axonal growth as being mediated via PKA, and inhibiting phosphodiesterase, the enzyme responsible for breaking down cAMP, coupled with embryonic spinal tissue implanted at the lesion site, has been shown to aid axonal regrowth after a spinal hemisection (Nikulina et al. 2004). Clearly the effect of cAMP with respect to axonal regeneration is not well understood. However, if a single molecule has been shown to have both inhibitory (astrocyte reactivity possibly leading to the formation of the glial scar) and positive effects with respect to axonal regrowth, perhaps the different downstream effectors are involved in completely separate functions and outcomes. This makes cAMP and its downstream effectors interesting subjects for regeneration studies.

Reactive astrocytes are not only an interest with respect to axonal regrowth; they also play a dual role in neurodegenerative disorders. In the case of multiple sclerosis, an autoimmune reaction against the myelin sheath leads to exposure of a naked axon. Reactive astrocytes near the degeneration protect the naked axon from secondary damage, but are also involved in glial scarring, which can present a physical barrier for remyelination of these axons. Although certain functions of reactive astrocytes protects insult sites from further damage, the consequences that result include failure to regain neuronal function.

In 1987, Malhotra and colleagues generated an antibody, monoclonal antibody J1-31 (mAb J1-31), against plaques of multiple sclerosis plaques, the antigen of which was detected more in reactive astrocytes than astrocytes in the quiescent phase and was described as being a more sensitive marker for reactive astrocytes than increased GFAP expression (Predy et al. 1988). The antigen of the monoclonal antibody was first characterized as distinct from GFAP (Predy et al. 1987). However, microscopy and western blotting techniques suggested the monoclonal antibody could indeed recognize GFAP, or possibly a variant of GFAP, as well as nuclear lamins (García et al. 2003). Since certain cytoskeletal components have been implicated as potential impediments to axonal regrowth following injury, the use of this more sensitive monoclonal antibody can be utilized to understand signaling pathways leading to their upregulation.

The F98 cell line is derived from a rat type IV astrocytoma, an astrocyte-derived tumor, and was used as a model for astrocytes in this study in alignment with the "replacement" element for reducing the use of animals in research in accordance with generally accepted guidelines. This study was undertaken to test the hypotheses that (1) cAMP is an important intracellular activator of pathways leading to astrocyte reactivity, and

(2) these pathways can be characterized using inhibitors of known cAMP effectors, namely

PKA and Epac. These hypotheses were tested by the use of commercially available

activators and/or inhibitors of PKA and Epac, which proved helpful in elucidating the

pathway responsible for the upregulation of the J1-31 antigen in astrocytes, utilizing the F98

cell line as a model.

CHAPTER II

MATERIALS AND METHODS

Cell Culture

Seeding From Frozen Cell Stocks

Frozen stocks of F98 cells (ATCC: CRL-2397) and J1-31 hybridoma (ATCC: CRL-2253) cell lines were stored in liquid nitrogen, courtesy of Dr. Gary Aron. Freezing media for the F98 cell line consisted of 90% growth media (see below) and 10% dimethyl sulfoxide (DMSO; Mallinckrodt: 4948), the cryoprotectant. The freezing media for the J1-31 hybridoma cell line consisted of 50% RPMI-1640 (ATCC: 30-2001), 40% fetal bovine serum (FBS; Sigma: F2442), and 10% DMSO.

All media and reagents were warmed to 37°C prior to cell exposure. Growth medium for the F98 cell line consisted of Dulbecco's Modified Eagle's Medium fortified with L-glutamine (ATCC: 30-2002), 10% FBS, and 0.5% penicillin/streptomycin (ATCC: 30-2300), which served to prevent growth of potential bacterial contaminants. The growth medium for the J1-31 hybridoma cell line consisted of RPMI 1640, 10% FBS, and 0.5% penicillin/streptomycin. The incubator conditions were set to 37°C, 5% CO_2, and was equipped with an humidifying aerator. Prior to introducing them to cells, all media were syringe-filtered drop wise through a 0.2 μm pore size filter (BioLink: BLTS22).

9

Cryovials containing cells were immediately placed in a water bath set to 37°C upon retrieval from the liquid nitrogen tank. Once heated, vial contents were added to 4 ml of fresh, warm, growth medium, centrifuged at 1200 rpm for five minutes in a tabletop centrifuge (International Equipment Company: AB4433), and the supernatant containing DMSO was discarded. Pellets were resuspended in 1 ml fresh media and transferred to a T-25 culture flask (BioLink: TP90026) containing 4 ml of warm growth media. Upon reaching confluency (2-3 days), F98 cells were detached using trypsin/EDTA (Gibco: R-001-100) and either split into new flasks with fresh medium, prepared for treatments, or frozen for storage.

Immunocytochemistry Preparation

Prior to seeding coverslips in preparation of cAMP treatments, F98 cells were allowed to undergo at least one round of splitting to allow ample time for adjusting to growth conditions after being frozen. Upon reaching confluency, cells were trypsizined and seeded onto 22 mm^2, ethanol sterilized coverslips placed within 35 mm^2 petri plates with an initial seeding density of 4.0 x 10^5 cells per cm^2, as determined using a hemocytometer (InCyto: DHC-N01-5). Cells were allowed to grow on coverslips for 72 hours in 3 ml of growth medium. Prior to treatments, old growth medium was replaced with warm, fresh media, and cells were allowed to adjust to fresh conditions for approximately one hour before initiation of treatments.

Source of mAb J1-31

J1-31 mouse hybridoma cells were grown under conditions as previously described for 48-72 hours. Upon completion of growth in culture, cells were either split or frozen down, and the old growth medium was stored as the source of mAb J1-31. Growth medium

from three T-75 (BioLink: TP90075) and four T-25 flasks of J1-31 cells was pooled and stored at -80°C prior to use. Sodium azide was added to a total of 0.05% prior to freezing to prevent growth of possible contaminants. The concentration of antibody remains unknown, as it is difficult to quantitate the presence of one particular protein in culture supernatants. Therefore, an immunocytochemical dilution series of culture supernatant was employed as a means to determine the appropriate amount of source antibody (results not shown).

mAb J1-31 Isotype Determination

mAb J1-31 was first characterized as an IgG2b isotype (Malhotra et al. 1989). However, ATCC lists mAb J1-31 as an IgM. In order to determine whether the hybridoma cell line produces IgG2b or IgM antibodies, or perhaps both, immunochemical procedures were performed to compare labeling with an anti-mouse IgG2b versus an anti-mouse IgM secondary antibodies. Immunocytochemistry, dot blots, and a monoclonal antibody isotyping kit were all utilized to ensure the appropriate secondary antibodies were used in subsequent experiments.

Cyclic AMP Pathway Treatments on F98 cells

Upon completion of the 72-hour growth in culture and media exchange, F98 cells were introduced to specific activators and inhibitors of downstream cAMP effectors. To elucidate which downstream effector is responsible for increased immunolabeling of mAb J1-31 and reactive phenotype, analogs of cAMP specific for PKA or Epac were introduced to cells growing on coverslips with concentrations and time courses listed in Table 2. The inhibitor specific for PKA used in this study was the potent, myristoylated, cell-permeant amide, 14-22 PKI. Treatments varying the concentration of the Epac activator, as well as

increasing the time course of treatment were also performed. The experimental negative

control employed cells on coverslips with no treatment. See Table 2 for more information.

Phosphodiesterase activity in our experimental model was also of interest. The Epac

activator has been described as having phosphodiesterase resistance, but no such description

of the PKA activator has been found in the literature. If the PKA activator were rapidly

degraded by phosphodiesterase, then the true effect of stimulating PKA would remain

unknown. In order to determine the actual effect stimulating PKA had on labeling of mAb

J1-31, phosphodiesterase was first inhibited with rolipram for ten minutes prior to

stimulating PKA. To determine the effects of sustaining cAMP levels over the one-hour

treatment period, phosphodiesterase was inhibited as previously described, followed by

forskolin treatment for one hour. The experimental vehicle negative controls for these

experiments were cells that had not been treated except for the addition of DMSO to a final

concentration of 0.33%, the solvent of both rolipram and forskolin. This was to ensure that

the effects of rolipram and forskolin treatments were not in fact due to DMSO.

Scratch Wounds

Scratch wound assays mimic mechanical trauma *in vitro* (Malhotra et al. 1995), and

were thus utilized to compare the phenotype of reactive cells versus cells in the quiescent

phase. Cells located along the scratch were expected to undergo reactive gliosis; therefore,

the phenotypes of such cells could be compared to cAMP pathway(s) treated cells in an

effort to generate a more pathologically relevant positive control. F98 cells were grown on

coverslips as previously described, and upon completion of 72 hours in culture and media

exchange, a 0.1-10 µl pipette tip was dragged across the center of the cell-containing

coverslips, thus detaching the cells located within the scratch wound. Cells were allowed to

grow on coverslips for an additional 24 prior to fixation and immunolabeling.

Fixation

Upon completion of treatments in culture, cell-bearing coverslips were briefly

washed in PBS (136.9 mM NaCl, 2.68 mM KCl, 10.14 mM Na_2HPO_4, and 1.76 mM

KH_2PO_4) warmed to 37°C and fixed in -20°C methanol for one minute. The methanol was

removed, and coverslips were allowed to air dry prior to procession of immunolabeling.

Immunocytochemistry

Methanol-fixed cells were first washed in PBS three times for 10 minutes each. To

prevent nonspecific primary antibody interactions, cells were blocked with 200 μl of 20%

nonfat dry milk (NFDM) diluted in PBS for two hours at room temperature, which was

followed by three PBS washes for 10 minutes each. Primary antibody incubation, 200 μl on

each coverslip, was performed overnight at 4°C. After incubating cells in primary antibody,

three 10 minute washes in PBS were performed, followed by a second blocking step in 200

μl of 20% NFDM for two hours at room temperature, followed by another round of washes.

Secondary antibody incubation, 200 μl on each coverslip, was then performed for two hours

at room temperature in the dark to prevent any loss of fluorescence. The secondary

antibody for mAb J1-31 was goat anti-mouse IgM conjugated to Texas Red. The secondary

antibody for anti-GFAP was chicken anti-rabbit IgG conjugated to Alexa Fluor 488 (AF

488). The negative controls for immunolabeling experiments were cell-bearing coverslips

that had been incubated with secondary antibody only. These negative controls ensured

results were not due to nonspecific binding of the secondary antibody. For double-staining

procedures, antibody cocktails, both primary and secondary, were prepared using the same

dilutions listed in Table 1. After the secondary antibody incubation, coverslips were washed three times in PBS for 10 minutes each. Coverslips were mounted on microscope slides using a small drop of 90% glycerol, and finger nail polish was spotted on the four corners to ensure potential sliding of the coverslips was eliminated. Note: in certain experiments, a nuclei stain, Hoechst (Invitrogen) diluted 1:2000, followed by three washes, was employed after the secondary antibody and consecutive washes.

Microscopy

Three X, Y, and Z- dimensional images were taken of each coverslip on an Olympus FV1000 confocal laser scanning microscope to ensure a sufficient sample size for statistical analysis. Each image consists of 22 optical slices 800 x 800 pixels (x,y dimensions) with a 0.3 μm step size (z dimension). Therefore, each z-projected image represented a 6.6 μm thickness on the z-axis. Each image was scanned at a speed of 40 μs/pixel, using the 559 nm laser for excitation of Texas Red fluor and/or the 488 nm laser for excitation of AF 488. Unless otherwise noted, each image was collected using the 60X oil immersion lens (numerical aperture (NA): 1.4). Each scale bar represents 30 μm.

Data Acquisition and Image Analysis

Using the FV1000 Olympus software, ten cells from each z-projected image were traced using the pencil tool (n=30 for each treatment). Cells that were physically in contact with other cells, whether directly adjacent or layered on one another, were excluded from selection (see Figure 12). Using the measurement tool, values for area and integrated pixel intensity for each region of interest (ROI) was obtained.

The degree of mAb J1-31 labeling can be quantified by calculating pixel intensity per unit area values for each ROI, and statistical inference procedures were performed on pixel intensity per unit area values. Program R was used to perform statistical procedures. Pixel intensity per unit area was first calculated in Excel, and the data were imported into program R. ANOVA was performed, followed by a Tukey's Honestly Significant Differences (HSD) multiple comparison procedure. Refer to Tables 3 4, and 5, respectively. A linear regression analysis was performed on the pixel intensity data for the Epac activator time course study (refer to Figures 6 and 7).

Table 1: Antibodies used in immunocytochemical analysis of cAMP effectors

Primary	Dilution in PBS	Secondary	Dilution in PBS
J1-31 hybridoma culture supernatant	1:2	Goat anti-mouse IgM conjugated to Texas Red (Santa Cruz Biotechnology sc-2983)	1:100
J1-31 hybridoma culture supernatant	1:2	Goat anti-mouse IgG2b conjugated to Texas Red (Santa Cruz Biotechnology sc-2781)	1:100
Rabbit anti-GFAP (SIGMA G9269)	1:100	Chicken anti-rabbit IgG conjugated to AlexaFluor® 488 (Invitrogen A-21441)	1:1000

Table 2: Specific activators and inhibitors of adenylyl cyclase and cAMP effectors

| Name	Target	Solvent	Working Concentration	Treatment Time Course
Forskolin (BIOMOL CN100)	Adenylyl cyclase	DMSO	4 μM	1 hour
8-CPT-2'-O-Me-cAMP sodium salt (Santa Cruz Biotechnology sc-202028)	Epac	H_2O	30 μM*	1 hour
6-Bnz-cAMP sodium salt (Sigma B4560)	PKA	H_2O	10 μM	1 hour
PKA inhibitor 14-22 amide (Calbiochem 476485)	PKA inhibitor	H_2O	36 nM	10 minutes
Rolipram (Sigma R6520)	Phosphodiesterase IV inhibitor	DMSO	88 nM	10 minutes/1 hour if alone

* The appropriate concentration was experimentally determined. See Figure 4.

CHAPTER III

RESULTS

Isotype Determination of mAb J1-31

In order to use the appropriate secondary antibody for mAb J1-31, it was first necessary to conclusively determine the isotype of the antibody produced by the J1-31 hybridoma cell line. The original discoverers of the monoclonal antibody reported the isotype to be an IgG2b. However, the product information sheet for the J1-31 hybridoma cell line lists the antibody as an IgM. Immunocytochemistry was performed with either goat anti-mouse IgG2b or goat anti-mouse IgM secondary antibodies, both conjugated to a Texas Red fluor, purchased from the same vendor, and used at the same working concentration. Staining untreated F98 cells with the same dilution of antibodies indicated a positive result with only anti-IgM secondary antibodies (see Figure 1). Upon this discovery, only anti-IgM secondary antibodies were used against the primary mAb J1-31.
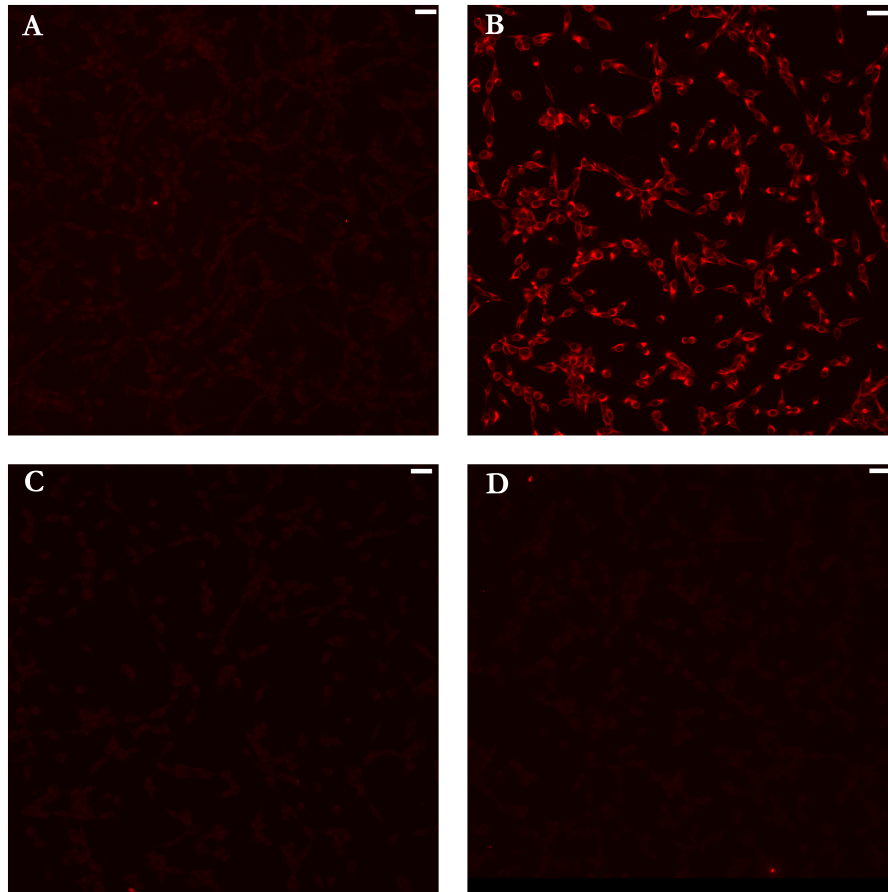
Figure 1. mAb J1-31 is a member of the IgM class of immunoglobulins. Untreated F98 cells were immunolabeled with mAb J1-31 and stained with either goat anti-mouse IgM conjugated to Texas Red (frame B) or goat anti-mouse IgG2b conjugated to Texas Red (frame D) secondary antibodies. Cells in frame A and C were not labeled with mAb J1-31, rather only the secondary antibody. Cells in frame A were only stained with goat anti-mouse IgM conjugated to Texas Red, and cells in frame C were only stained with goat anti-mouse IgG2b conjugated to Texas Red. Each image was taken with a 20X dry objective lens (NA: 0.75). Each scale bar represents 30 μm. After observing a positive result exclusively with the goat anti-mouse IgM, only this secondary antibody was used in subsequent experiments.

cAMP Effector Treatments

Although cAMP is involved in a wide range of signaling pathways, only three known downstream targets are known. Analogs of cAMP specific for either PKA or Epac are commercially available, as well as inhibitors of PKA. To elucidate the effector(s) of cAMP responsible for the increased immunodetection of the J1-31 antigen, F98 cells were treated targeting specific pathways, followed by a comparison of pixel intensity values of 30 cells from each treatment. Increased immunolabeling with mAb J1-31 is apparent after treating F98 cells with forskolin, stimulating Epac, or a combination of the two with PKA inhibition (see Figures 2 and 3).

A significant difference among treatments was observed, with a p value << 0.001 (See Table 3). In order to determine the differences among treatments, a Tukey's Honestly Significant Difference (HSD) post hoc test was performed. Again, significant differences were detected. In summary, cells treated with forskolin, the Epac activator, or mixtures of the two with PKI, the PKA inhibitor, did not significantly differ from one another, but all showed significantly greater pixel intensities than cells that had not been treated, or cells treated only with the PKA activator only. The results of this study led to optimization studies with the Epac activator.
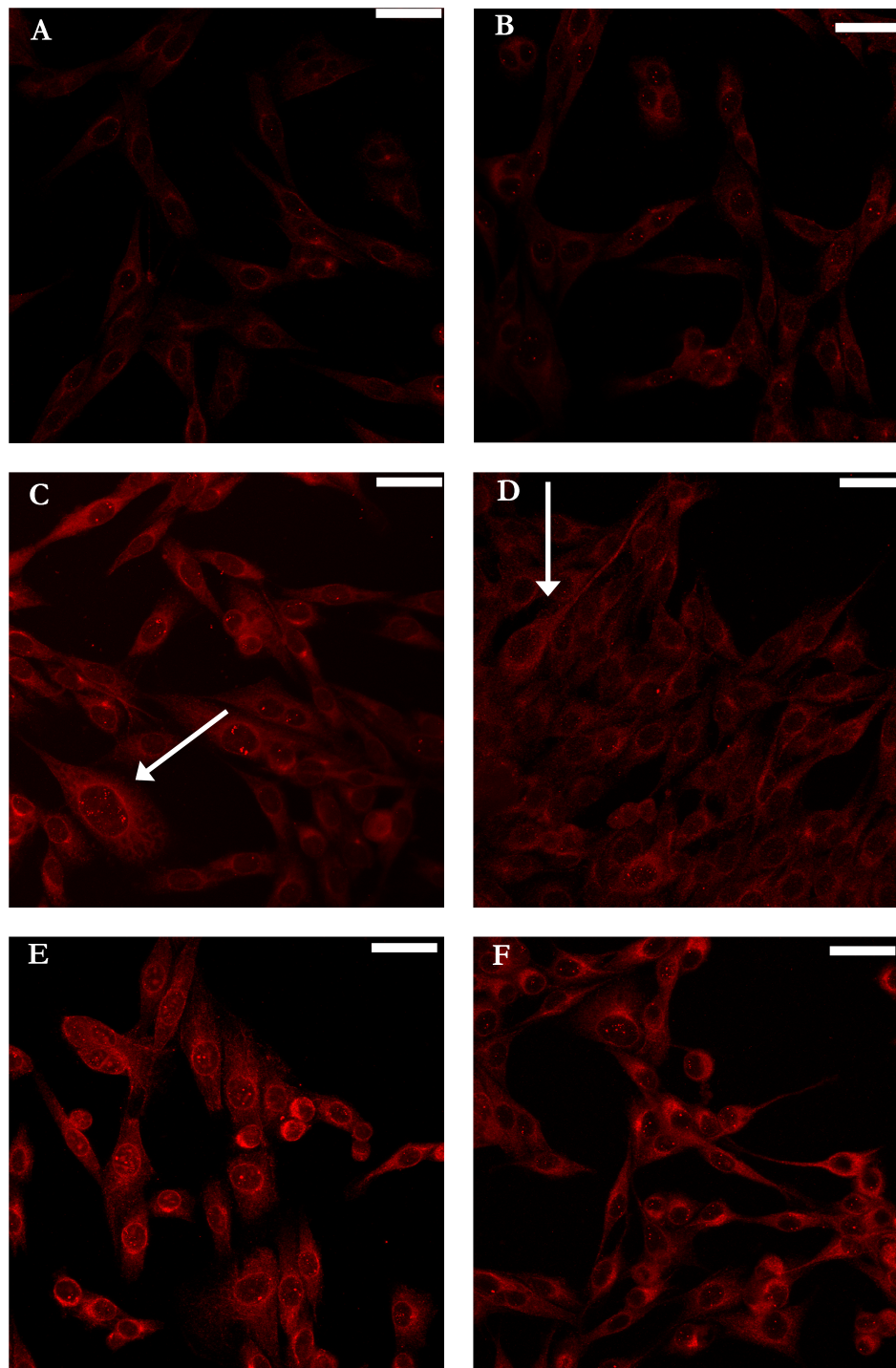
Figure 2. Increased mAb J1-31 labeling is dependent on activation of Epac, not PKA. Cells in frame A were untreated. Cells in frame B were treated with the PKA activator, cells in frame C were treated with the Epac activator, and cells in frame D were treated with forskolin. Cells in frames E and F were initially treated with PKI followed by treatment with the Epac activator or forskolin, respectively. Each image was acquired with a 60X oil immersion lens (NA: 1.40), arrows indicate reactive cells, and each scale bar represents 30 μm. Significant differences among treatments were detected (p << 0.001).
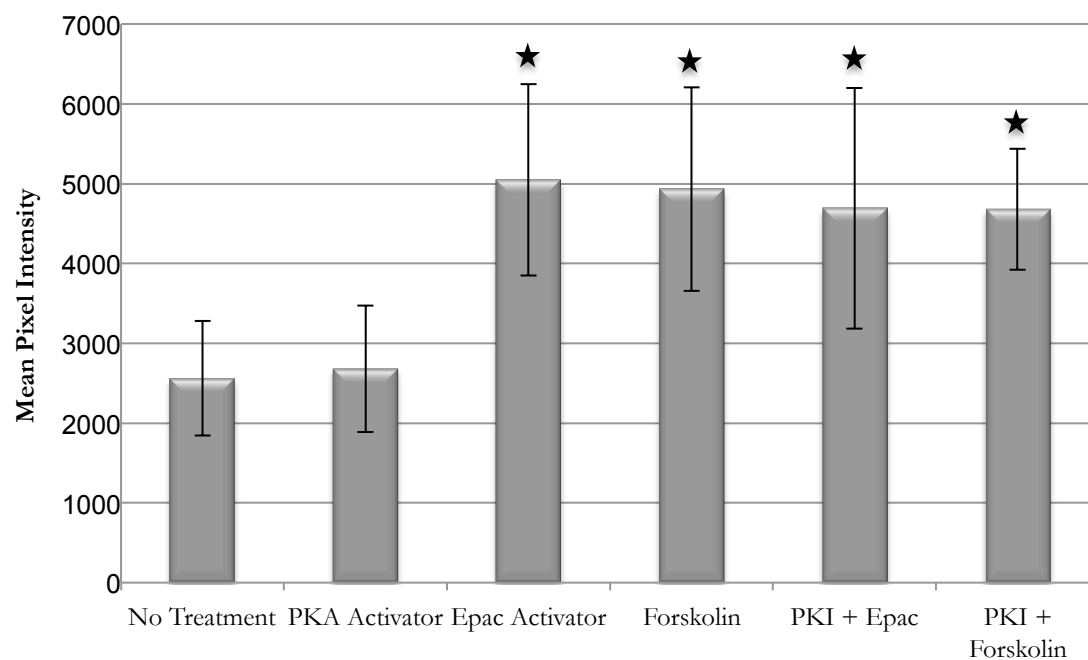
Figure 3. Bar graph representation of pixel intensity values for each treatment discussed in Figure 2. Means and standard deviations of pixel intensity values per treatment were calculated in Excel, and this bar graph was generated. Significance was detected in pixel intensity values for treatments indicated with a star. Although no significance was detected, the decreased pixel intensity values for treatments with PKI was slightly less than treatments without, which may be due to errors in ROI data selection.

Table 3. ANOVA table generated from R after analyzing the cAMP effector study.
After calculating pixel intensity per unit area values for 30 cells per treatment (cells from
Figure 2), data was imported into program R, and an ANOVA was calculated. With an F
statistic value of 33.886 on 5 and 174 degrees of freedom, a significant p value was detected,
therefore indicating there was indeed a difference among treatments. Upon obtaining a
significant p value, a Tukey's HSD test was performed to determine how the treatments
compared with one another.

|	Df	Sum Sq	Mean Sq	F Value	P value
cAMP Treatments	5	199375547	39875109	33.886	<<0.001
Residuals	174	204751474	1176733		

**Epac Activator Concentration and Time Course Studies**

Initial results of cAMP treatments revealed that treatments either inhibiting PKA while elevating levels of cAMP or activating Epac led to the highest degree of mAb J1-31 labeling. To determine the conditions under which increased labeling due to Epac activation were maximal, treatments with increasing time course and concentration of the Epac activator were performed. If stimulating Epac indeed leads to increase labeling of mAb J1-31 and reactive phenotype, then increased mAb J1-31 labeling was expected with increasing concentration and treatment time course. Treatments with Epac activator ranging from 10 μM to 40 μM revealed labeling patterns suggesting saturation kinetics (see Figure 4). Between 30 μM and 40 μM, there appears to be a saturation point, where a lessened mAb J1-31 labeling effect was seen in 40 μM treated cells (See Figure 4). Indeed, cells treated with 30 μM Epac activator had significantly higher pixel intensity values than all other treatments (refer to Figures 4 and 5). It is also pertinent to note that some cells that were treated with 40 μM of the Epac activator began detaching from the coverslip during the course of treatment. After this study, the concentration of the Epac activator used was 30 μM.

Upon determining the appropriate concentration of the Epac activator, a time course study was performed. If Epac is indeed the effector of cAMP responsible for the increased immunodetection of the J1-31 antigen, then increased mAb J1-31 labeling was expected with increasing time of treatment with the Epac activator. This was indeed evident, as illustrated in Figure 6. A linear regression was analyzed using the same data acquisition procedures as described previously, and a significant p value was detected ($p << 0.001$). The Pearson's product moment correlation coefficient, which was used to test the degree of correlation between the two variables, was 0.741 (see Figure 6). The Pearson's product moment

correlation coefficient ranges from -1 to +1 and measures the strength of dependence of two variables. With a highly positive correlation (0.741), this result further supports the notion that Epac is the cAMP effector involved in the reactive response.
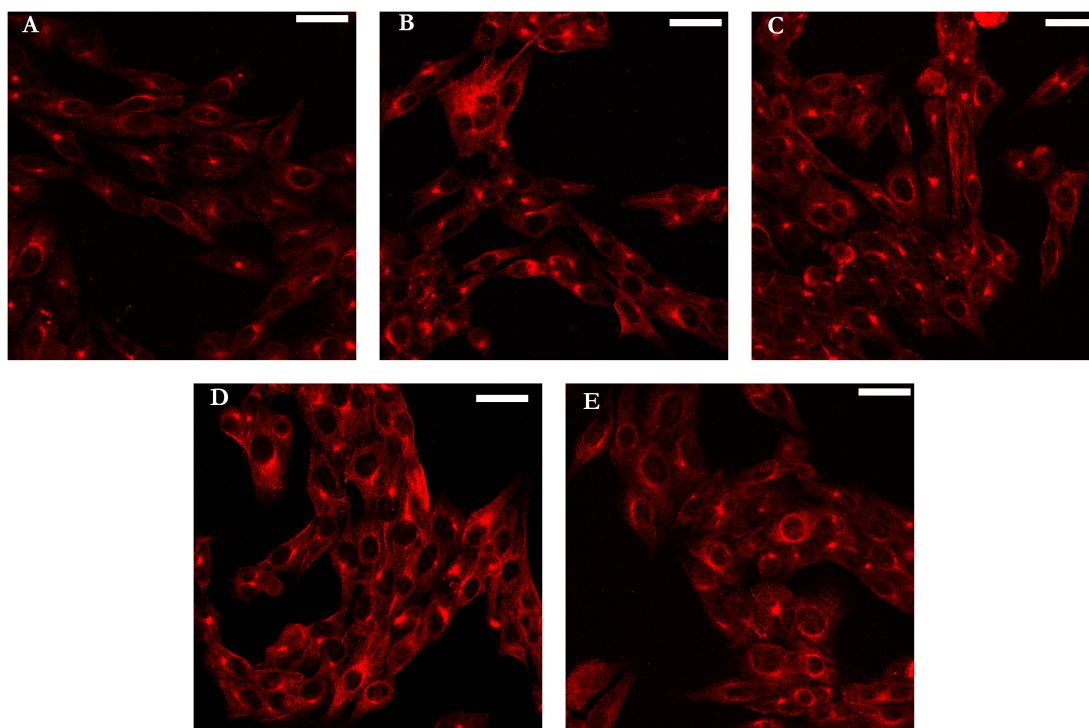
Figure 4. Epac activator dose response study. In order to determine the appropriate concentration of the Epac activator that leads to the highest degree of mAb J1-31 labeling and reactive phenotype, F98 cells were seeded and treated as previously described. Cells were treated with 10 μM, 15 μM, 20 μM, 30 μM, and 40 μM 8-CPT-O-Me-cAMP, respectively for 20 minutes. Cells treated with 30 μM 8-CPT-O-Me-cAMP had the highest degree of mAb J1-31 labeling, and remained adhered to the coverslip. Many cells treated with 40 μM 8-CPT-O-Me-cAMP began to detach from the coverslip prior to completion of treatment. Thus for subsequent studies, the Epac activator concentration was 30 μM. Each scale bar represents 30 μm, and each image was acquired with a 60X oil immersion lens (NA: 1.40).
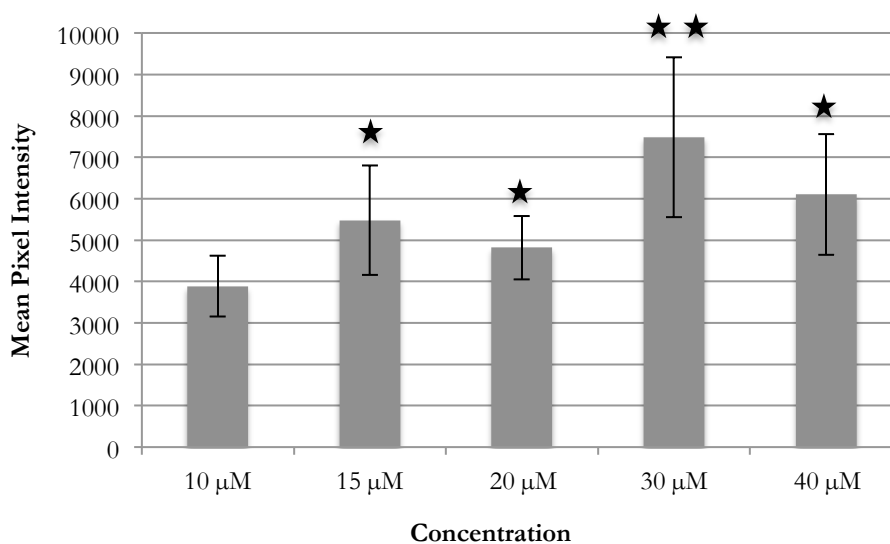
Figure 5. Bar graph representation of pixel intensity values for each treatment discussed in Figure 4. Means and standard deviations of pixel intensity values per treatment were calculated in Excel, and this bar graph was generated. Treatments indicated with one star indicate significantly higher pixel intensity values when compared to the no treatment, and the treatment marked with two stars indicates significant differences than all the other treatments. The decrease (although no significance was detected) between 15 μM and 20 μM may be attributed to errors in data acquisition.

Table 4. ANOVA table generated from R after analyzing the Epac activator dose response study. After calculating pixel intensity per unit area values for 30 cells per treatment (cells from Figure 4), data was imported into program R, and an ANOVA was calculated. With an F statistic value of 28.3 on 4 and 135 degrees of freedom, a significant p value was detected, therefore indicating there was indeed a difference among treatments. Upon obtaining a significant p value, a Tukey's HSD test was performed to determine how the treatments compared with one another.

	Df	Sum Sq	Mean Sq	F Value	P value
cAMP Treatments	4	180842225	45210556	28.326	<<0.001
Residuals	135	215474084	1596104		
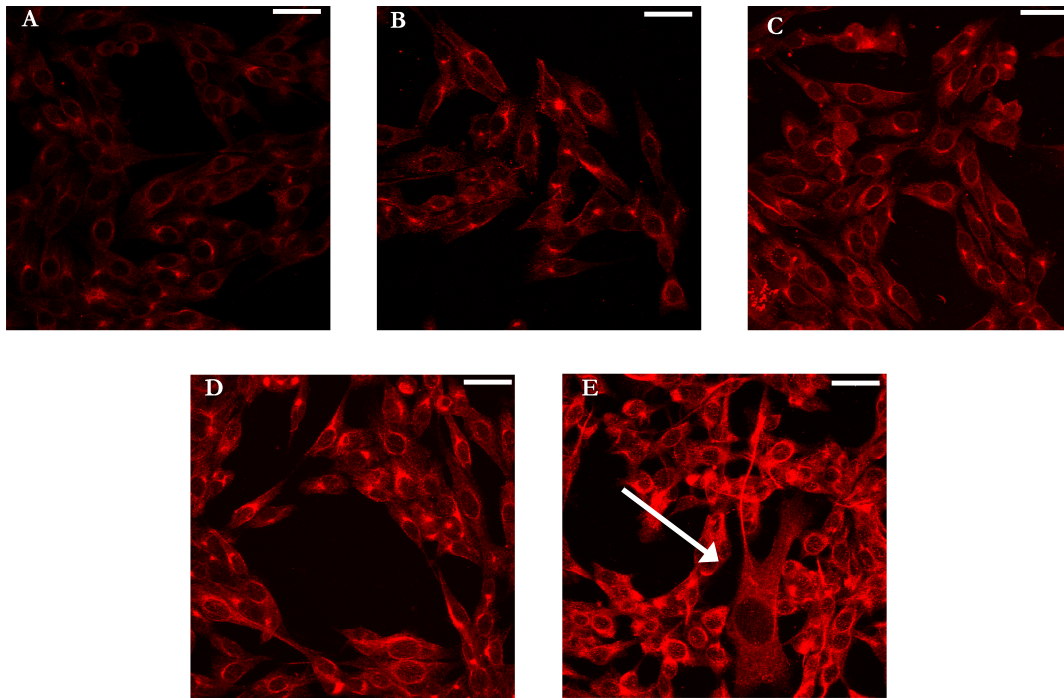
Figure 6. Increasing the treatment time course of the Epac activator reveals a linear trend in mAb J1-31 labeling. In order to determine the effects of stimulating Epac over increasing periods of time, cells in frames A-D were treated with 30 μM Epac activator for periods of 10, 20, 30, and 60 minutes. Cells in frame E were treated with 30 μM Epac activator for 24 hours. However, since this experiment was performed with cells from a different flask of cells, pixel intensity values for these cells were not included in the statistical analysis. The inclusion of this image was for qualitative purposes only. Each scale bar represents 30 μm, the white arrow indicates a reactive phenotype, and each image was taken with a 60X oil immersion lens (NA: 1.40). A linear regression analysis was performed, a significant p value was detected ($p \ll 0.001$), and the Pearson's moment correlation coefficient was 0.741.
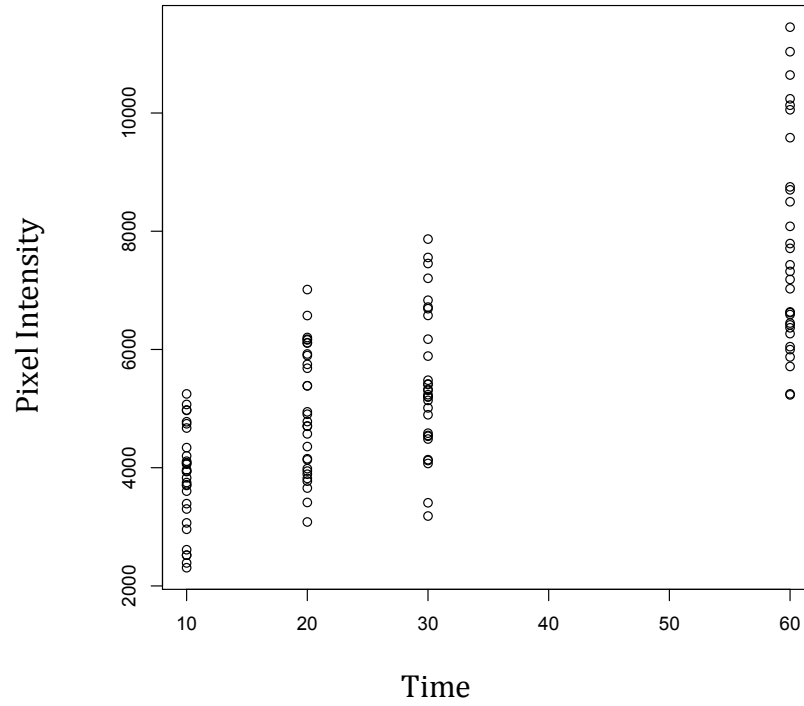
Figure 7. Plot of time versus pixel intensity from the Epac activator time course study. The R-squared value was 0.5486, with an F-statistic value of 143.4 on 119 degrees of freedom, which leads to a p-value<< 0.001 (from cells in Figure 6). The Pearson's product-moment correlation coefficient was 0.741.

Phosphodiesterase Study

The activity of phosphodiesterase, the enzyme responsible for breaking down cAMP, was of interest in this study. The cAMP analog specific for Epac has been described as having some phosphodiesterase resistance, but no such resistance as been reported regarding the cAMP analog specific for PKA. Unless phosphodiesterase is inhibited, the true effect of stimulating PKA would remain unknown in this model since the analog could be degraded before the effects of PKA stimulation could be discerned. Conveniently, there are also commercially available inhibitors of phosphodiesterase, and the inhibitor used in this study was rolipram. Rolipram is a type IV phosphodiesterase inhibitor, and was used in this study because astrocytes are known to express type IV phosphodiesterases (Borysiewicz et al. 2009).

F98 cells were first treated with rolipram for ten minutes followed by treatments with forskolin, the Epac activator, or the PKA activator. Data acquisition, an ANOVA, and a Tukey's HSD test were performed as previously described. In summary, the same trend of results was apparent (see Figures 8 and 9). Phosphodiesterase inhibition followed by stimulating with forskolin or Epac revealed pixel intensity values that were statistically greater than the vehicle no treatment, rolipram only, or rolipram followed by PKA activation, which did not significantly differ from one another (see Table 5 for ANOVA table).
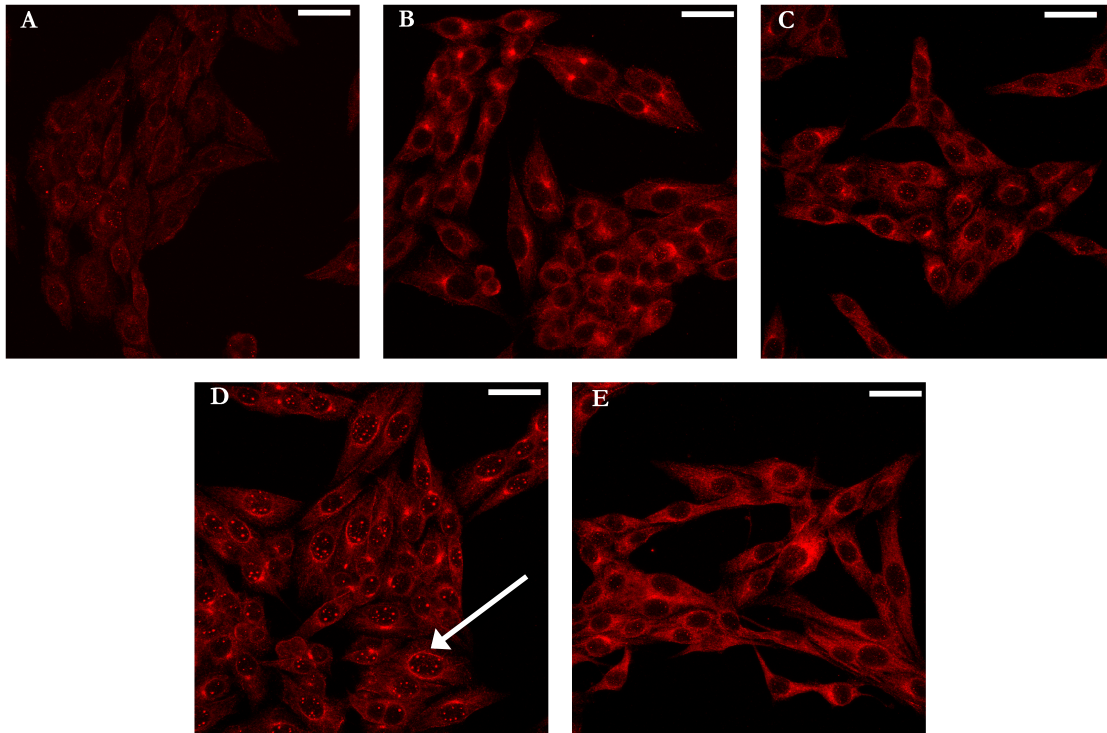
Figure 8. Inhibiting phosphodiesterase does not reveal a role for PKA in increased mAb J1-31 labeling. In order to determine the true effect of the PKA activator, rolipram, a phosphodiesterase inhibitor, was first introduced to cells prior to a one-hour activator treatment period. Cells in frame A were exposed to growth medium containing 0.33% DMSO to serve as the vehicle control. Cells in frame B were treated with rolipram for one hour. Cells in frames C, D, and E were first treated with rolipram for ten minutes followed by one-hour treatments with the PKA activator, the Epac activator, or forskolin, respectively. When comparing cells in frame D to previous studies with the Epac activator, a lessened effect is seen. This may be attributed to potential loss of stability of the Epac activator over time. However, a significant difference among treatments was still detected ($p \ll 0.001$). Each image was acquired with a 60X oil immersion lens, the white arrow indicates a hypertrophic cell, and each scale bar represents 30 μm.

Table 5. ANOVA table generated from R after analyzing the phosphodiesterase study. After calculating pixel intensity per unit area values for 30 cells per treatment (cells from Figure 8), data was imported into program R, and an ANOVA was calculated. With an F statistic value of 30.128 on 4 and 145 degrees of freedom, a significant p value was detected, therefore indicating there was indeed a difference among treatments. Upon obtaining a significant p value, a Tukey's HSD test was performed to determine how the treatments compared with one another.

	Df	Sum Sq	Mean Sq	F Value	P value
PDI Treatments	4	126668317	31667079	30.128	<<0.001
Residuals	145	152407425	1051086		
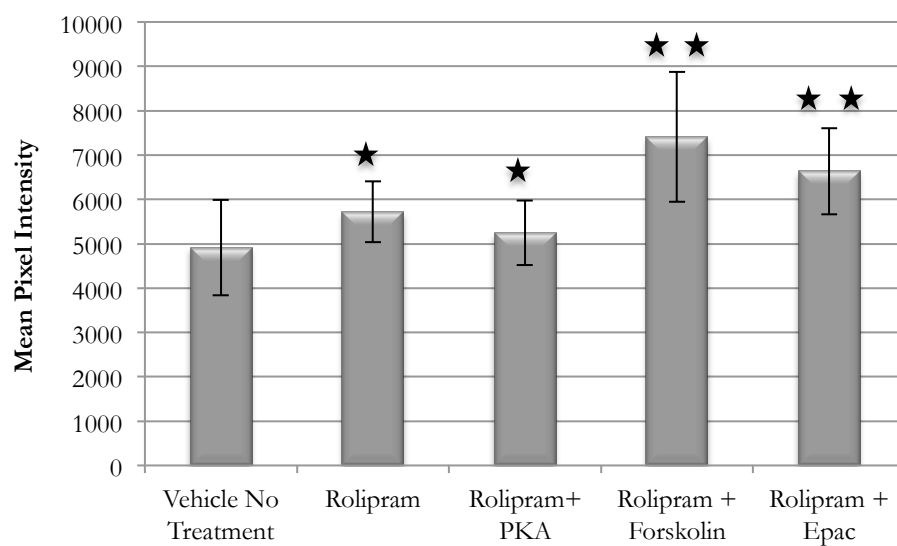
Figure 9. Bar graph representation of pixel intensity values for each treatment discussed in Figure 8. Means and standard deviations of pixel intensity values per treatment were calculated in Excel, and this bar graph was generated. Pixel intensity values for treatments indicated with one star were significantly greater than the vehicle no treatment. Pixel intensity values for treatments indicated with two stars were significantly greater than the other treatments.

Colocalization Study with mAb J1-31 and anti- GFAP

Western blotting analyses reveal mAb J1-31 recognizes proteins with relative molecular masses characteristic of nuclear lamins (~65 kD), GFAP (~45 kD), and periodically a 32 kD fragment is evident (data not shown and García et al. 2003). In order to determine if mAb J1-31 recognizes GFAP, or a variant of, a colocalization study with anti-GFAP and mAb J1-31 was performed (see Figure 10). It was also of interest to determine how stimulating Epac affected labeling of both antibodies. F98 cells with no treatment were compared to cells that had been treated with the Epac activator.
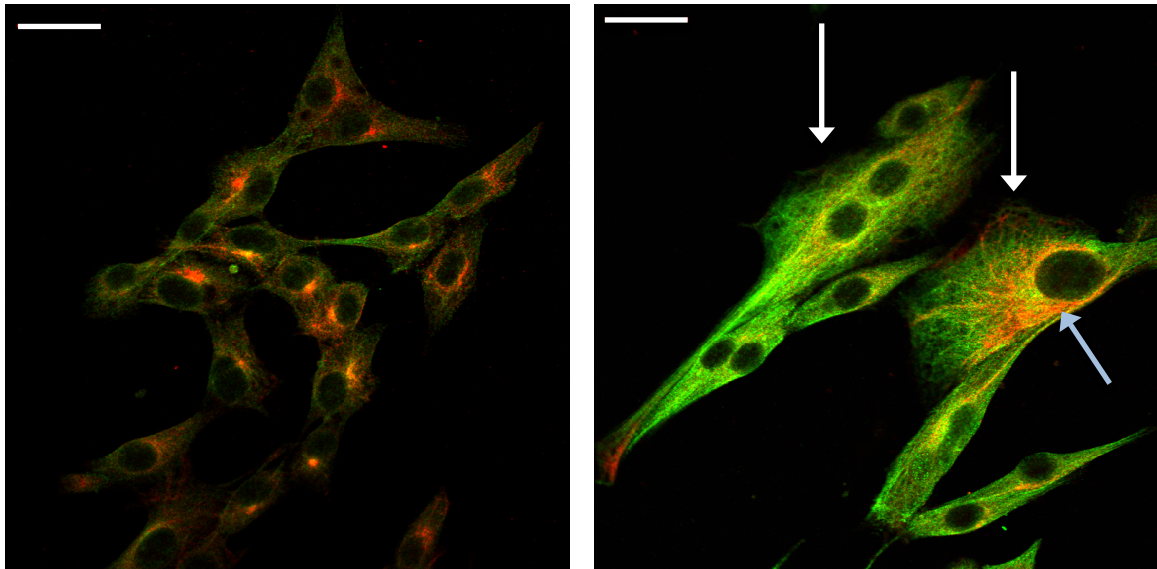
Figure 10. Anti-GFAP and mAb J1-31 reveal incomplete colocalization, and stimulation of Epac reveals increased labeling of both. In order to determine if there is colocalization between the J1-31 antigen and GFAP, and whether Epac stimulation causes an increase of immunolabeling of both, double staining procedures were performed. Green represents labeling of GFAP, and red represents labeling of the J1-31 antigen. Cells in the left frame were untreated, and cells in the right frame were treated with 30 μM Epac activator for one hour. Note the hypertrophic phenotype of cells on the right, along with the increase of brightness in both the red and the green channels. There appears to be incomplete colocalization between GFAP and J1-31 (blue arrow), which may indicate the epitope differences of the two antibodies on GFAP. Each image is a single optical slice, scale bars represents 30 μm, white arrows indicate hypertrophic cells, and each image was acquired with a 60X oil immersion lens (NA: 1.40).

Scratch Wounding

Scratch wound assays have been used as a means to induce reactivity by mimicking mechanical trauma *in vitro* (Malhotra et al. 1995). Dragging a micropipette tip across a relatively thick monolayer of cells detaches cells within the scratch, and cells located along the scratch wound undergo reactive gliosis, the beginning stage in the development of a glial scar. If mAb J1-31 were truly a marker for reactive astrocytes, then it would be expected for cells located nearest the scratch wound to have the highest degree of labeling. Frame by frame viewing of a scratch wound assay in Figure 11 appears to support this prediction. The cells located along the periphery of the scratch wound, as well as cells located within the scratch, appear to be more hypertrophic, with a higher degree of mAb J1-31 labeling, than cells with increasing distance from the scratch (see Figure 11). Scratch-induced reactive F98 cells shared phenotypic features in common with cells treated with the Epac activator (see Figures 2 and 11).
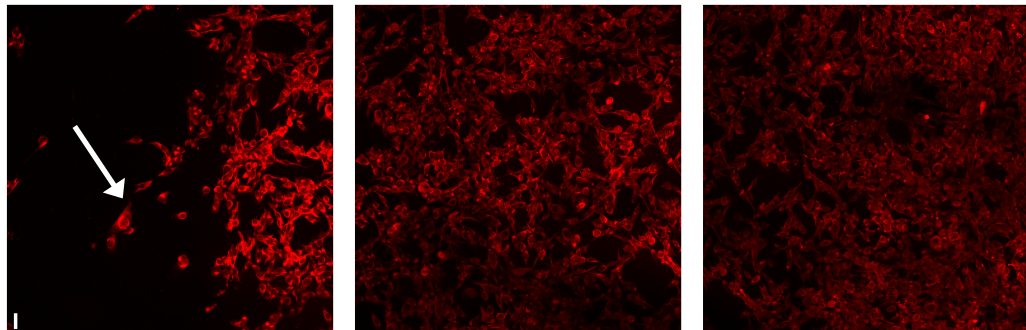
Figure 11. Frame-by-frame view of a scratch wound at 20X magnification. Scratch wound assays were utilized as a means to induce mechanical reactivity *in vitro*. F98 cells were seeded onto coverslips as previously described, and upon reaching confluency, a scratch wound assay was performed, followed by immunolabeling with mAb J1-31. Note the labeling pattern of mAb J1-31 and reactive phenotype exhibited by cells nearest to the scratch wound (indicated with arrow), as well as the lessened effect seen with increasing distance from the scratch. Each image represents 1024 x 1024 pixels, which converts to 212 μm x 212 μm. Therefore, the three consecutive frames represent roughly 640 μm. The scale bar represents 30 μm, and each image was acquired using a 20X dry lens (NA: 0.75).

CHAPTER IV

DISCUSSION

Isotype Discrepancy of mAb J1-31

Malhotra first characterized mAb J1-31 to be an IgG2b isotype (Malhotra et al. 1989). However, when obtaining the J1-31 hybridoma cell line from ATCC, the product information sheet listed mAb J1-31 as an IgM. F98 cells immunolabeled with mAb J1-31, stained with either goat anti-mouse IgG2b or goat anti-mouse IgM produced by the same vendor at the same concentration reveals a positive result exclusively when stained with the anti-IgM secondary antibody (see Figure 1).

Perhaps the J1-31 hybridoma initially started as a mixed culture of IgG and IgM producing hybridoma cells, and culture conditions selected for IgM producing cells, an idea Dr. Marsha Wills-Karp suggested at the 2011 Women in Science and Engineering conference at Texas State University-San Marcos. Interestingly, Predy et al. (1987) discussed using either goat anti-mouse IgG or IgG +IgM secondary antibodies for mAb J1-31, but did not discuss why the polyvalent secondary antibody was used. Although perplexing as to why the isotype either switched from an IgG2b to an IgM or perhaps both were present in the initial hybridoma culture, labeling patterns of mAb J1-31 in this study reveal similar labeling patterns and localization as former studies (see for example García et al. 2003). It is important to note a former student, Mya Patel, performed dot blots using the J1-31 culture

supernatant with an anti-IgG secondary antibody, and culture supernatants collected prior to 2003 revealed a positive result under those conditions, and culture supernatants from J1-31 cells purchased after this time revealed a negative result (data not shown).

Phenotypic Analysis

As a means to mechanically induce trauma *in vitro*, scratch wound assays served as an experimental positive control. When observing cells treated with the activators of downstream targets of cAMP, those treated with the Epac activator, forskolin, or mixtures of the two with PKI most closely resemble cells nearest the scratch wound with respect to mAb J1-31 labeling patterns and phenotypes (see Figures 2, 4, 6, 8, and 11).

The hypertrophic response has been described as cell enlargement increased stellations, or both (Daginakatte et al. 2007, Sofroniew and Vinters 2010). Within close proximity to the scratch wound, examples of both cell enlargement (hypertrophy) and increased stellation are evident (see Figure 11). Cells treated with PKI followed by treatment with forskolin or the Epac activator seem to be less hypertrophic, but with increased number of stellations compared to cells with forskolin or the Epac activator alone (see Figure 2). These results suggest either there is a role for PKA in the hypertrophic response or hypertrophy and increased stellations occur via separate mechanisms. To ascertain whether there is indeed a role for PKA in the reactive response, future experiments could examine expanding the parameters of the PKA activator used in this study, e.g. through dose response and time course studies, as well as inhibiting PKA for the duration of a scratch wound assay.

Signaling Pathway Connections

The downstream target of Epac is Rap1, a small GTPase that has been characterized as having involvement in cell adhesion, formation of gap junctions, and promoting ERK/MAPK pathway phosphorylation (Holz et al. 2006). Considering the formation of the glial scar involves the formation of overlapping processes (stellations) belonging to reactive astrocytic (Sofroniew and Vinters 2010), conceptually the involvement of Rap1 in this formation makes sense. Astrocytes are known to express integrins, and studies have shown an upregulation of such adhesion molecules in neurodegenerative diseases (Milner et al. 1999). The experimental evidence of this study suggests the hypertrophic reactive response is mediated by Epac; therefore, it follows that Rap1 may be mediating the overlapping, adhesive effect seen in the glial scar.

Recall the initial hypothesis of this study was that PKA is the kinase responsible for phosphorylating an epitope on GFAP and nuclear lamins, forming putative J1-31 antigen. Activation of PKA in this system, however, did not yield an increase of mAb J1-31 labeling (see Figures 2, 3, 8, and 9). Perhaps the ERK/MAPK signaling cascade, which is activated following Epac stimulation (Holz et al. 2006), includes the kinase responsible for phosphorylating GFAP and nuclear lamins. Furthermore, the activation of the MAPK signaling pathway has been shown in astrogliosis (Carbonell and Mandell 2003), which can also be traced back to the involvement of Rap1 and Epac.

GTPases have been implicated in regulating morphological changes in astrocytes (Buffo, Rolando, and Ceruti, 2009), and the upregulation of a Rho GTPase has been correlated with cytoskeletal rearrangements indicative of reactive astrocytes (Abbracchio et al. 1997). The present study supports the inference that the downstream target of Epac,

Rap1, may be one of these GTPases involved in these reported cytoskeletal rearrangements involved in the transition of astrocytes to the reactive state.

Studies have shown that neurite outgrowth is dependent on PKA and not Epac (Wan et al. 2011), and certain researchers have reported cAMP to be involved in promoting axonal regrowth after injury (Cai et al. 1999, Nikulina et al. 2004). It is certainly interesting that two downstream effectors of one signaling molecule can promote nearly opposite functions, one being axonal regrowth and the other the astrocyte hypertrophic response, as seen in this study, which is the beginning process of an inhibitory action with respect to neuronal regrowth after injury.

Summary and Future Directions

In summary, the conclusion of this study is that Epac, and not PKA, is involved in the transition of astrocytes to the cAMP-dependent reactive state based on the parameters used in this study, namely increased J1-31 labeling and hypertrophy. Perhaps activation of one effector of cAMP can be utilized to promote axonal regrowth after CNS injury (PKA), while the activity of another effector promoting the astrocytic hypertrophic response can be inhibited (Epac). Monoclonal antibody J1-31 has shown to be a useful tool in characterizing the reactive response, and it recognizes cytoskeletal components, namely GFAP among others, that are (1) upregulated during the reactive response and (2) considered a culprit behind the lack of regenerative capabilities of higher vertebrates.

For continuing projects on this study, I propose looking into Epac inhibition with brefeldin, for example, as well as optimizing the PKA activator treatments. I also propose incorporating *in vivo* treatments to observe the effects of PKA or Epac inhibition on CNS regeneration after injury. Furthermore, the reactive response leading to the different aspects

of the changing phenotype of reactive astrocytes, namely hypertrophy or stellated

morphology, should be further explored.
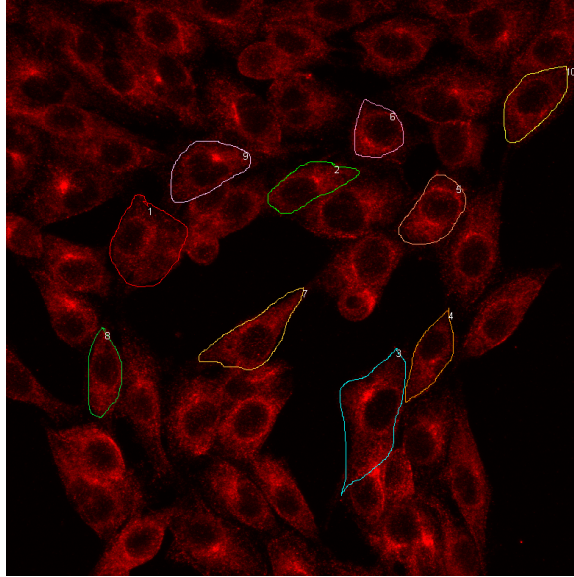
Figure 12. Example of data acquisition. F98 cells in z-projected images were traced using the FV1000 software's pencil tool (n=30 per treatment) prior to statistical analyses. This image was acquired with a 60X oil immersion objective lens (NA: 1.40).

REFERENCES

Abbracchio, M., Rainaldi, G., Giammarioli, A.M., Ceruti, S., Brambilla, R., Cattabeni, F., et al. (1997). The A_3 adenosine receptor mediates cell spreading, reorganization of actin cytoskeleton, and distribution of Bcl-XL: studies is human astroglioma cells. *Biochemical and Biophysical Research Communications, 241*(2), 297-304.

Borysiewicz, E., Fil, D., Diaboga, D., O'Donnell, J.M., & Konat, G.W. (2009). Phosphodiestearse 4B2 gene is an effector of Toll-like receptor signaling in astrocytes. *Metab Brain Dis, 24*(3), 481-491.

Buffo, A., Rolando, C., & Ceruti, S. (2010). Astrocytes in the damaged brain: molecular and cellular insights into their reactive response and healing potential. *Biomedical Pharmacology, 79*(2), 77-89.

Cai, D., Qiu, J., Cao, Z., Actee, M., Bregman, B., & Filbin, M. (2001). Neuronal cyclic AMP controls the developmental loss in ability of axons to regenerate. *J. Neurosci., 21*(13), 4731-4739.

Carbonell, S.W., & Mandell, J.W. (2003). Transient neuronal but persistent astroglial activation of ERK/MAP kinase after focal brain injury in mice. *Journal of Neurotrauma, 20*(4), 327-336.

Daginakatte, G.C., Gadzinski, A., Emnett, R.J., Stark, J.L., Gonzales, E.R., Yan, et al. 2007. Expression profiling identifies a molecular signature of reactive astrocytes stimulated by cyclic AMP or proinflammatory cytokines. *Experimental Neurology, 20*(1), 261-267.

Fang, D., Li, Z., Zhong-ming, Q., Mei, W.X., Ho, Y.W., Yuan, X.W. et al. (2008). Expression of bystin in reactive astrocytes induced by ischemia/reperfusion and chemical hypoxia in vitro. *Biochim Biophys Acta, 1782*(11), 658-663.

Faulkner, J.R., Herrmann, J.E., Woo, M.J., Tansey, K.E., Doan, N.B., & Sofroniew, M.V. (2004). Reactive astrocytes protect tissue and preserve function after spinal cord injury. *J Neurosci, 24*(9), 2143-2155.

Fedoroff, S., McAulley, W.A., & Houkle, J.D. (2004). Astrocyte cell lineage. V. Similarity of astrocytes that form in the presence od dBcAMP in cultures to reactive astrocytes in vivo. *Journal of Neuroscience Research, 12*(1), 15-27.

García, D.M., Weigum, S.E., & Koke, J.R. 2003. GFAP and nuclear lamins share an epitope recognized by monoclonal antibody J1-31. *Brain Research, 976*(1), 9-21.

Geisert, E.E., Johnson, H.G., & Binder, L.I. (1990). Expression of microtubule-associated protein 2 by reactive astrocytes. *Proc. Natl. Sci. USA, 87*(10), 3967-3971.

Giulian, D., & Lachman, L.B. (1985). Interleukin-1 stimulation of astroglial proliferation after brain injury. *Science, 228*(4698), 497-499.

Grafstein, B., Liu, S., Cotrina, M. L., Goldman, S.A., & Nedergaard, M. (2000). Meningeal cells can communicate with astrocytes by calcium signaling. *Annals of Neurology, 47*(1), 18-25.

Hausmann, R., Riess, R., Fieguth, A., & Betz, P. (2000). Immunohistochemical investigations on the course of astroglial GFAP expression following human brain injury. *Int J Legal Med, 113*(2), 70-75.

Haydon, P.G., & Carmignoto, G. (2006). Astrocyte control of synaptic transmission and neurovascular coupling. *Physiol Rev, 86*(3), 1009-1031.

Holz, G.G., Kang, G., Harbeck, M., Roe, M.W., & Chepurny, O.G. (2006). Cell physiology of cAMP sensor Epac. *Journal of Physiology, 577*(1), 5-15

Janzer, R.C., & Raff, M.C. (1987). Astrocytes induce blood-brain barrier properties in endothelial cells. *Nature, 325*(1), 253-257.

Lee, R.K.K., Araki, W., & Wurtman, R. (1997). Stimulation of amyloid precursor protein synthesis by adrenergic receptors coupled to cAMP formation. *PNAS, 94*(10), 5422-5426.

Malhotra, S.K., Bhatnagar, R., Shnitka, T.K., Herrera, J.J., Koke, J.R., & Singh, M.V. (1995). Rat glioma cell line as a model for astrogliosis. *Cytobios, 82*(328), 39-51.

Malhotra, S.K., Predy, R., Johnson, E.S., Singh, R., & Leeuw, K. (1989). Novel astrocytic protein in multiple sclerosis plaques. *Journal of Neuroscience Research, 22*(1), 36-49.

Malhotra, S.K., Svensson, M., Aldskogius, H., Bhatnagar, R., Das, G.D., & Shnitka, T.K. (1993). Diversity among reactive astrocytes: Proximal reactive astrocytes in lacerated spinal cord preferentially react with monoclonal antibody J1-31. *Brain Research Bulletin, 30*(3-4), 395-404.

Menet, V., Prieto, M., Privat, A., & Gimenez y Ribotta, M. (2003). Axonal plasticity and functional recovery after spinal cord injury in mice deficient in both glial fibrillary acidic protein and vimentin genes. *PNAS, 100*(15), 8999-9004.

Milner, R., Huang, X., Wu, J., Nishimura, S., Pytela, R., Sheppard, D. et al. (1999). Distinct roles for astrocyte αvβ5 and αvβ8 integrins in adhesion and migration. *Journal of Cell Science, 112*, 4271-4279.

Myer, D.J., Gurkoff, G.G., Lee, S.M., Hovda, D.A., & Sofroniew, M.V. Essential protective proles of reactive astrocytes in traumatic brain injury. (2006). *Brain, 129*(10), 2761-2772.

Neve, L.D., Savage, A.A., Koke, J.R., & García, D.M. (2011). Activating transcription factor 3 and reactive astrocytes following optic nerve injury in zebrafish. *Comp Biochem Physiol C Toxicol Pharmacol, 155*(2), 213-218.

Nikulina, E., Tidwell, J.L., Dai, H.N., Bregman, B.S., & Filbin, M.T. (2004). The phosphodiesterase inhibitor rolipram delivered after a spinal cord lesion promotes axonal regeneration and functional recovery. *PNAS, 11*(23), 8786-8790.

Pekny, M., Camilla, E., Siushansian, R., Ding, M., Dixon, S.J., Pekna, M. et al. (1999). The impact of genetic removal of GFAP and/or vimentin on glutamine levels and transport of glucose and ascorbate in astrocytes. *Neurochemical Research, 24*(11), 1357-1362.

Predy, R., Malhotra, S.K., & Das, G.D. (1988). Enhanced expression of a protein antigen (J1-31 antigen, 30 kilodaltons) by reactive astrocytes in lacerated spinal cord. *Journal of Neuroscience Research, 19*(4), 397-404.

Predy, R., Singh, D., Bhatnagar, R.S., & Malhotra, S.K. (1987). A new protein (J1-31 antigen, 30 kD) is expressed by astrocytes and ependymal. *Bioscience Reports, 7*(6), 491-502.

Saul, K.E., Koke, J.R., & García, D.M. (2010). Activating transcription factor 3 (ATF3) expression in the neural retina and optic nerve of zebrafish during optic nerve regeneration. *Comp Biochem Physiol A Mol Integr Physiol, 155*(2), 172-182.

Silver, J., & Miller, J.H. (2004). Regeneration beyond the glial scar. *Nat Rev Neurosci, 5*(2), 146-156.

Sofroniew, M.V. 2005. Reactive astrocytes in neural repair and protection. *Neuroscientist, 11*(5), 400-407.

Sofroniew, M.V., & Vinters, H.V. (2010). Astrocytes: biology and pathology. *Acta Neuropathol, 119*(1), 7-35.

Takanaga, H., Yoshitake, T., Hara, S., Yamaskaki, C., & Kunimoto, M. (2004). cAMP-induced astrocytic differentiation of C6 glioma cells is mediated by autocrine interleukin-6. *J Biol Chem, 279*(15), 15441-15447.

Tetzlaff, W., Graeber, M.B., Bisby, M.A., & Kreutzberg, W. (1988). Increased glial fibrillary acidic protein synthesis in astrocytes during retrograde reaction of the rat facial nucleus. *Glia, 1*(1), 90-95. *The Journal of Neuroscience 21*(4), 1257-1264.

Tokita, Y., Keino, H., Matsui, F., Aono, S., Ishiguro, H., Higashiyama, S., and Oohira, A. (2001). Regulation of neuregulin expression in the injured rat brain and cultured astrocytes.

Yiu, G. & He, Z. (2006). Glial inhibition of CNS axon regeneration. *Nature Reviews Neuroscience, 7*(1), 617-627.

VITA

Sarah Jo Kane was born in Colorado Springs, Colorado, on June 14, 1988 to Kevin and Kari Kane. She was raised in Divide, Colorado until moving to Texas in 1998, where she graduated high school from Bremond High School. Sarah attended Texas State University-San Marcos from 2006-2010 after being awarded a Texas State Excellence Scholarship (formerly known as the Mitte Scholarship). She graduated *summa cum laude* in December 2010 with a B.S. in biology and a minor in chemistry, and decided to pursue a master's degree under the supervision of Dr. Joseph Koke. Sarah's research aims to understand a cell type that is partially responsible for the lack of central nervous system regenerative capabilities in mammals. She has particular interest in understanding the role of these cells in neurodegenerative diseases such as multiple sclerosis.

Permanent Address: PO Box D
                     Bremond, TX 76629

This thesis was typed by Sarah J. Kane.